A PHASE VELOCITY ANALYSIS OF MULTIGRID METHODS FOR HYPERBOLIC EQUATIONS

W. L. WAN * AND TONY F. CHAN †

Abstract. In this paper, we study the effects of coarse grid correction (CGC) on multigrid convergence for hyperbolic problems in one and two dimensions. We approach this from the perspective of phase velocity, which allows us to exploit the hyperbolic nature of the underlying PDE. In particular, we consider three combination of coarse grid operators and coarse grid solution approaches: (1) Runge-Kutta smoothing CGC, direct discretization, (2) exact coarse grid solve, direct discretization, and (3) Galerkin CGC. For all these approaches, we show that the convergence behavior of multigrid can be precisely described by the phase velocity analysis of the coarse grid correction matrix, and we verify our results by numerical examples in one and two dimensions.

1. Introduction. Multigrid has been a powerful and successful numerical technique for fast solution of elliptic partial differential equations (PDEs). Many different approaches have been proposed and various sophisticated techniques have been developed for the cases of nonsmooth coefficient PDEs, complex geometries and unstructured meshes (see, for example, [3, 18, 31, 34] and survey in [13]). For the elliptic case, multigrid convergence is governed by smoothing of the high frequencies and coarse grid correction of the smooth frequencies. Classical Fourier analysis [3, 18, 34] and finite element analysis [2, 18, 36] have been well developed. However, this principle may not hold for the hyperbolic case since the success of the standard techniques often rely on the intrinsic properties of elliptic PDEs, for instance, symmetry, decay of Green's function and dissipation, which are not generally true for hyperbolic problems.

Several smoothing techniques have been proposed for convection dominated problems. One approach is to apply Gauss-Seidel with the so-called downwind ordering [1, 10, 19, 25, 33]. Another approach is to use time-stepping methods as smoothers [20, 21, 24, 27]. The idea is that this class of smoothers do not just reduce the high frequency errors, but more importantly, also propagate the errors along the flow directions. Typically, the coarse grid correction is done by a few smoothing steps. Thus, the multigrid process can be interpreted as speeding up the wave propagation by taking larger time step sizes on the coarse grids. As a result, errors can be removed rapidly by propagating them out of the boundary. A detailed summary of recent multigrid developments for nonelliptic PDEs can be found in [9].

Fourier analysis has been a useful tools for analyzing multigrid methods and more generally, iterative methods [14]. A simplified but more generally applicable version, the local mode analysis, can be obtained by considering an infinite grid, i.e. ignoring the boundary effect. It was first introduced to analyze multigrid smoothing and two-level analysis by Brandt [3] and was later extended in [5, 6, 7, 8]; see also [18, 30, 31, 34]. In the half-space mode analysis [5, 6], the boundary effect can also be studied. For non-elliptic problems, first differential approximation (FDA) analysis [4] is often used to analyze smooth components. In this analysis, the discrete differential operator is replaced by its first differential approximation [37], and the intergrid transfer and smoothing operators are ignored. For a model convection-diffusion equation with very small diffusion coefficient, it has been shown in [4, 11, 12] that the two-level convergence factor is at best 0.5. Fourier analysis of multigrid methods for convection dominated problems can also be found in [17, 29, 34]. Although two-level analysis is often sufficient to determine convergence behavior, occassionally, three-level analysis is necessary [35].

For hyperbolic equations, one must also take into account the intrinsic wave propagation property

* Department of Computer Science, University of Waterloo, Waterloo, ON, Canada N2L 3G1. Email: jwlwan@math.uwaterloo.ca. This author was supported by the Natural Sciences and Engineering Research Council of Canada, and partially by the NSF grant ACI-0072112.

† Department of Mathematics, University of California at Los Angeles, Los Angeles, CA 90095-1555. Email: chan@math.ucla.edu. The author has been partially supported by the NSF under contract ACI-0072112 and DMS-9973341.

(phase speed) for analyzing multigrid convergence. Phase velocity has been used extensively to analyze numerical methods for hyperbolic problems [32] but its use in the context of multigrid has not been much explored. We are advocating such an approach in this paper.

In the classical Fourier analyses mentioned above, the emphasis was primarily on the spectral radius estimates. For elliptic problems, the spectral radius is often an accurate measure of multigrid efficiency. However, it is not necessarily true for hyperbolic equations. For instance, suppose Jacobi iteration (cf. (6)) is used to solve the linear wave equation (5) with $\Delta t/\Delta x = 1$. Then the spectral radius of the Jacobi iteration matrix is 0, but the convergence is slow (N steps in general). Thus, to analyze the efficiency of the wave propagation multigrid approach, the classical Fourier analysis is not adequate as it ignores completely the phase speeds, which account for the wave propagation. Gustafsson and Lötstedt [16, 26] first analyze the phase speed of this multigrid approach, and prove that a speedup of $2^K - 1$ in convergence is obtained using K grids for smooth errors, which would not be inferred from the spectral radius analysis.

In practice, however, the multigrid convergence can be much slower than the analysis predicts due to severe numerical oscillations generated by the algorithm (cf Section 2). In the analysis of Gustafsson and Lötstedt, they focus primarily on the leading order term of the asymptotic expansion of the phase speed. In this paper, we extend their analysis to include also the first order correction term with which we can explain the dispersive behavior of the multigrid process which turns out to have significant influence on the convergence rate.

We find that the phase velocity analysis is not just useful for the wave propagation multigrid approach but it can also be used to explain the efficiency of other coarse grid correction methods as well. One common coarse grid correction approach is to use the discretization matrices as the coarse grid operators on the coarse grids. It has been shown by Brandt and Yavneh in [4, 11, 12, 38] that the resulting coarse grid correction has O(1) error for the Fourier components in the characteristic direction. Our phase velocity analysis not only recovers the same result, but also provides more insight into the source of the error. In particular, we prove that this coarse grid correction is only first order accurate for components in the cross-characteristic direction due to the phase shift error caused by the discretization coarse grid operators.

In this paper, we show that the Galerkin coarse grid correction [28, 39] can be a more efficient approach from the perspective of phase error. We prove that the phase shift error of the coarse grid correction is smaller than that of the previous approach, and hence higher order accuracy of the coarse grid correction can be achieved. We note, however, that Galerkin coarse grid operators tend to become central difference discrete operators which may lead to spurious oscillations in the coarser grid calculations. To remedy this problem, Dendy [15] uses operator-dependent restriction and linear interpolation. Yavneh [38] also uses interpolation and restriction operators which depend on the flow directions, together with artificial viscosity. He also pointed out that the order of accuracy of the high frequency components is crucial to obtain efficient Gakerlin coarse grid correction. Based on our phase velocity analysis, one should use the Galerkin approach with an appropriately defined interpolation so that the Galerkin coarse grid operator is stable, for instance, the same as the one by direct discretization. However, how to construct such an interpolation requires sustantial investigation and is not within the scope of this paper.

We would like to note that the FDA analysis [4] assumes that the effect of the inter-grid transfer operators is negligible on the convergence of the smooth components, and hence it is completely ignored. However, as reported in [4, page 84], downwind residual transfer is observed to produce better convergence results, which was not explained. In fact, different interpolation and restriction operators lead to very different phase errors of the coarse grid correction process. In section 5, we demonstrate how our phase velocity analysis can successfully prove the fast convergence of two multigrid methods using upwind-type interpolation and restriction, which the FDA analysis would have concluded that convergence rate cannot be better than 0.5.

In the rest of the paper, we shall study the effects of coarse grid correction on multigrid convergence for hyperbolic problems in one and two dimensions. In particular, we consider three combination of coarse grid operators and coarse grid solution approaches. For all these methods, we show that the convergence behavior of multigrid can be precisely described by the phase velocity analysis of the coarse grid correction matrix.

In Section 3, explicit analytic formulae for the asymptotic expansion of the phase velocity of the different coarse grid correction approaches are established in one dimension. In Section 4, similar results in two dimensions are presented with the emphasis on Fourier components in the characteristic and cross characteristic directions. Numerical results are given in Section 6 to compare how these coarse grid correction approaches affect the actual multigrid convergence. Finally, concluding remarks are given in Section 7.

2. Model problem. The model problem we are interested in is the steady state solution of linear hyperbolic equations:

$$Lu(x) \equiv \sum_{i=1}^{d} a_i(x) \frac{\partial u}{\partial x_i} = f(x) \qquad x \in \Omega,$$

subject to periodic boundary conditions. Here, $a_i(x)$ are smooth functions, and Ω is a d-dimensional unit cube.

Discretizing the equation by finite difference methods on a standard uniform fine grid Ω^h on Ω with mesh size h results in a linear system

$$L^h u^h = f^h.$$

We consider solving the discrete problem using K grids, $\{\Omega^l\}_{l=0}^{K-1}$, where the finest grid is $\Omega^{K-1} = \Omega^h$, and Ω^{l-1} is obtained from Ω^l by standard full coarsening. Denote by p^l the prolongation operator from Ω^{l-1}, and by r^l the restriction operator from Ω^l to Ω^{l-1}, $l = 1, 2, \ldots, K-1$. Also, denote the smoothing operator on Ω^l by S^l, and q steps of smoothing by $S_l^{(q)}$. The solution process on the coarsest grid is denoted by CGC (coarse grid correction).

A standard multigrid V-cycle algorithm with q_1 steps of presmoothing and q_2 steps of postsmoothing can be written as [3, 18]:

procedure MG(l,u,f)
if $l = 0$
  $u = \mathrm{CGC}(u, f)$;
else
  $u = S_l^{(q_1)}(u, f)$;
  $d = r^l(L^l u - f)$;
  $v = 0$;
  $\mathrm{MG}(l-1, v, d)$;
  $u = u - p^l v$;
  $u = S_l^{(q_2)}(u, f)$;
end
  $u = u^n$;
  $\mathrm{MG}(K-1, u, f)$;
  $u^{n+1} = u$;

In the approach analyzed by Gustafsson and Lötstedt [16, 20, 27], the coarse grid correction used is: $CGC = S^{(q_1+q_2)}(u, f)$. The idea is to accelerate wave propagation on the coarse grids. Note that for hyperbolic equations, it is often useful to interpret the smoothing process as solving a pseudo time dependent problem:

$$\frac{\partial u^l}{\partial t} + L^l u^l = f^l \qquad l = 0, 1, \ldots, K-1. \tag{1}$$

It is well-known that dissipation and dispersion are two fundamental quantities for analyzing time stepping methods. Consider the one dimensional linear wave equation

$$u_t + a u_x = 0. \tag{2}$$

Given a finite difference scheme, suppose the Fourier transform of the numerical solution at time step $n+1$ can be written as

$$\hat{u}^{n+1}(\mu) = g(\mu)\hat{u}^n(\mu),$$

where $g(\mu)$ is the amplification factor and μ is the wave number.

Definition: The scheme is dissipative if $|g(\mu)| < 1$, and it is dispersive if the phase velocity [32], $\kappa(\mu)$, defined as,

$$\kappa(\mu) \equiv -\frac{\arg(g(\mu))}{\mu\pi\Delta t},$$

is different for different wave number μ, where Δt is the time step size. The phase velocity, $\kappa(\mu)$, measures the propagation speed of the wave with wave number μ.

Thus, the classical multigrid analysis using Fourier analysis is deemed to be inadequate since it only considers the dissipation property. To give a more precise account of the wave propagation property of the multigrid V-cycle which is considered as one time-stepping method, Gustafsson and Lötstedt [16, 26] analyzed the phase velocity of the multigrid process by a Fourier analysis of the two-grid iteration matrix M, which, in the case of m-stage Runge-Kutta smoothing, can be written as $M = CS$, where the coarse grid correction matrix, C, and the iteration matrix of the smoother, S, are given by

$$\begin{aligned} C &= I - p(L^H)^{-1}((I - \sum_{j=1}^{m}(\Delta t_H L^H)^j \prod_{k=m-j+1}^{m}\alpha_k) - I)rL^h \\ S &= I - \sum_{j=1}^{m}(\Delta t_h L^h)^j \prod_{k=m-j+1}^{m}\alpha_k. \end{aligned}$$

Let $\hat{M}$ be its Fourier transform. It is well-known [18, 34] that $\hat{M}$ is block diagonal with 2×2 subblocks $\hat{M}_\mu$ where $\mu = 0, \ldots, N-1$ are the Fourier modes (cf Section 3). We summarize the results of the analysis of Gustafsson and Lötstedt as follows:

THEOREM 2.1. *Let λ_1 be the first eigenvalue of $\hat{M}_\mu$. For frequency $\mu \approx 0$,*

$$\lambda_1(\mu) = 1 - (\Delta t_h + \Delta t_H)i\mu\pi + O(\mu^2).$$

Consequently, the phase velocity of the two-grid method is

$$\kappa(\mu) = -\frac{\arg(\lambda_1(\mu))}{\mu\pi\Delta t_h} = 1 + \frac{\Delta t_H}{\Delta t_h} = 3.$$

In general, if t_l denotes the time step on grid l, then the phase speed of the K-level multigrid method is given by,

$$\kappa(\mu) = \frac{1}{\Delta t_1}\sum_{j=1}^{K}\Delta t_j = 2^K - 1, \qquad \mu \approx 0.$$

Hence, the smooth errors should propagate out of the boundary with a speed of $2^K - 1$. However, as it turns out, the effective speed of wave propagation is much slower than the analysis predicts. The reason is that their analysis focuses primarily on the leading order terms of the Taylor expansion of λ_1 which only accounts for the speed of propagation of smooth waves. However, as noted in Section 3, relaxation smoothing for hyperbolic equations is not as effective as for elliptic dominated equations. Thus, error after smoothing also consists of nonnegligible higher frequency modes which need to be taken into account.

As an example, we take a square wave as the starting vector, which consists of nonnegligible high frequency Fourier modes. Snap shots of the error in the first sixty multigrid V-cycles are shown in

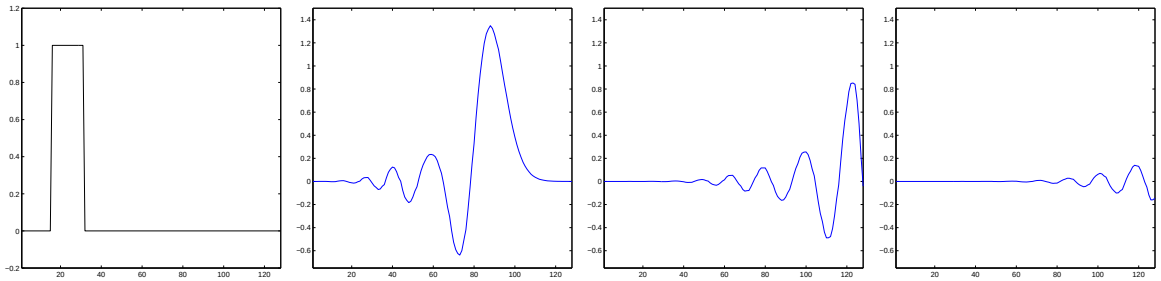

FIG. 1. *The numerical solutions given by a 3-level multigrid V-cycle at (a) iteration = 0, (b) iteration = 20, (c) iteration = 40, (d) iteration = 60.*

Figure 1. We use linear interpolation, one step of Euler smoothing, and 3 coarse grids. The number of fine grid points is 128. For $\lambda = 0.5$, the single grid method (i.e. only smoothing) will converge in 256 iterations. The analysis of Gustafson and Lötstedt estimated that the multigrid method should have a speedup of $2^3 - 1 = 7$, and it should have converged in 36 iterations. However, it takes more than 100 iterations to reduce the initial residual norm by 10^{-6}. The reason is that, as shown in Figure 1, oscillations are generated as the wave propagates to the right and they delay convergence.

3. One dimension. In this case, we establish explicit analytic formula for the Taylor expansion of the phase velocity which accounts for the effectiveness of coarse grid corrections. The model problem becomes:

$$u_x = f(x) \qquad -1 < x < 1$$

with periodic boundary condition: $u(-1) = u(1)$. On a uniform grid $\{x_j^h\}_{-N \le j \le N-1}$ with mesh size h, the standard upwinding discretization results in a linear system:

$$L^h u^h = f^h,$$

where

$$(L^h u^h)_i = \frac{u_i^h - u_{i-1}^h}{h}, \tag{3}$$

$u^h = (u_{-N}^h, \ldots, u_{N-1}^h)$, $u_j^h \approx u(x_j^h)$, and f^h is defined similarly as u^h. As in the classical analysis of multigrid for linear elliptic PDEs, without loss of generosity, we assume that $f^h \equiv 0$. Thus, we are interested in how the iteration error converges to zero.

Let the coarse grid points $\{x_j^H\}_{-N/2 \le j \le N/2-1}$ be obtained by standard coarsening, i.e. $x_j^H = x_{2j}^h$. For simplicity, assume the two-grid method consists of one pre-smoothing followed by the coarse grid correction (no post-smoothing). Then the iteration matrix M of the two-grid method can be written as

$$M = CS,$$

where C and S are the iteration matrices of the coarse grid correction and the smoothing, respectively.

Denote the discrete Fourier function (mode) by ψ_μ^h:

$$\psi_\mu^h(x_j^h) = \frac{1}{\sqrt{2N}} e^{i\mu\pi x_j^h} \qquad -N \le \mu \le N-1.$$

We note that ψ_μ^h, $|\mu| \approx 0$, correspond to smooth or less oscillatory modes whereas ψ_μ^h, $|\mu| \approx N$, correspond to the most oscillatory modes. The orthogonal Fourier transform matrix Q_h can be formed by taking ψ_μ^h as its columns. For two-grid analysis, it is customary to pair up the low and high frequency modes as follows [18, 34]:

$$Q_h = [\psi_0^h \;\; \psi_{-N}^h \;\; \psi_1^h \;\; \psi_{-N+1}^h \;\; \cdots \;\; \psi_{N-1}^h \;\; \psi_{-1}^h].$$

Define the Fourier transformed matrix $\hat{M}$ by

$$\hat{M} \equiv Q_h^{-1} M Q_h,$$

and similarly for other Fourier transformed matrices. For instance,

$$\hat{L}_\mu^h = \begin{bmatrix} 1 - e^{-\mu\pi hi} & \\ & 1 + e^{-\mu\pi hi} \end{bmatrix}, \qquad \mu = 0, 1, \ldots, N-1, \tag{4}$$

for the discretization matrix L^h in (3).

3.1. Analysis of smoothers. Smoothing by time-stepping methods approach is based on the discretization of the pseudo-time dependent problem:

$$u_t + u_x = 0. \tag{5}$$

Any numerical methods for solving (5), in principle, can be used as smoothers for multigrid, for instance, Runge-Kutta [20, 22], Lax-Wendroff [27], etc. For easy exposition, we consider the first order Euler's method where the smoothing step can be written as

$$u_i^{n+1} = u_i^n - \frac{\Delta t}{\Delta x}(u_i^n - u_{i-1}^n). \tag{6}$$

We remark that it coincides with the Richardson relaxation smoothing for solving $L^h u^h = 0$. Let $\lambda = \Delta t/\Delta x$ be the CFL number. The Fourier transform of Euler's method is given by:

$$\hat{u}_\mu^{n+1} = (1 - \lambda + \lambda e^{-\mu\pi hi})\hat{u}_\mu^n \equiv g(\mu\pi h)\hat{u}_\mu^n, \tag{7}$$

where $g(\mu\pi h)$ is the amplification factor.

The value of Δt (or equivalently λ) must satisfy the CFL condition so that the Runge-Kutta smoothing does not diverge. However, the choice of a particular value seems arbitrary. In [20], Jameson chose the largest possible Δt satisfying the CFL condition locally to maximize wave propagation. The analysis in [16] used the same choice. We note that the effectiveness of the smoothers in reducing the high frequency errors depends on the choice of Δt (or λ). For instance, when $\lambda = 1$, $\hat{u}^{n+1}$ becomes:

$$\hat{u}^{n+1} = e^{-\mu\pi hi}\hat{u}^n. \tag{8}$$

That is, error components of any frequency are not reduced at all. In fact, it is well-known that when $\lambda = 1$, it is an exact integration of (5), i.e. all waves are propagated exactly without smoothing and with the same speed. In general, for $0 < \lambda < 1$, by direct calculation, we have

$$|g(\mu\pi h)|^2 = 1 - 4\lambda(1-\lambda)\sin^2(\frac{\mu\pi h}{2}).$$

Thus, it is dissipative of order 2 for $0 < \lambda < 1$ with maximum dissipation when $\lambda = 0.5$, in which case,

$$g(\mu\pi h) = \frac{1}{2} + \frac{1}{2}e^{-\mu\pi hi}, \quad |(g\mu\pi h)| = \cos(\frac{\mu\pi h}{2}) \equiv c_\mu.$$

Compared to the smoothing factor of Richardson relaxation smoothing applied to the Poisson equation where

$$|g(\mu\pi h)| = \cos^2(\frac{\mu\pi h}{2}) = c_\mu^2,$$

Euler's smoothing for hyperbolic equation is less effective in damping high frequency Fourier modes, $\mu \approx N$.

We remark that Jameson [20] avoids the effect of Δt on the smoothing efficiency by using a different set of parameters for high order Runge-Kutta methods in such a way that high frequency components

are damped, assuming maximum Δt is used. We also note that Ni [27] and Gustafson and Lötstedt [16] use artificial dissipation (viscosity) to damp the high frequency components.

Consider again the case $\lambda = 1$ for our model problem. We have $|g(\mu\pi h)| = |e^{-\mu\pi h}| = 1$. The classical Fourier smoothing analysis would have concluded that this is not a robust smoother [34], and hence would not predict fast multigrid convergence. However, the phase velocity of $g(\mu\pi h) = 1$, and therefore the error is propagated by one grid point, with no dissipation. In general, for $0 < \lambda < 1$, the phase angle, θ, of $g(\mu\pi h)$ is given by

$$\tan\theta = \frac{\lambda \sin(\mu\pi h)}{1 - 2\lambda \sin^2(\frac{\mu\pi h}{2})}.$$

For the low frequency Fourier modes, i.e., $\mu\pi h \approx 0$, by Taylor expansion, we have

$$\theta(\mu\pi h) = \lambda\mu\pi h[1 - (\frac{1}{6} - \frac{\lambda}{2} + \frac{\lambda^2}{3})(\mu\pi h)^2 + O(\mu\pi h)^4].$$

By definition, the phase velocity is:

$$\kappa(\mu) = \frac{\theta(\mu\pi h)}{\lambda\mu\pi h} = 1 - (\frac{1}{6} - \frac{\lambda}{2} + \frac{\lambda^2}{3})(\mu\pi h)^2 + O(\mu\pi h)^4.$$

Since the correct phase velocity is 1, the method is dispersive of order 2 for $\mu\pi h \approx 0$.

Hence, in the following, we assume that the smoothers are some time stepping schemes which are dissipative and perhaps also dispersive. As the main theme of this paper, we shall consider three types of coarse grid correction approaches for hyperbolic equations commonly used in the literature. The first one is "Runge-Kutta coarse grid correction" where the coarse grid problem is solved inexactly by a few Runge-Kutta smoothing steps and the coarse grid operator is obtained by direct discretization. This is also the same approach considered by Gustafsson and Lötstedt [16], and others [20, 27]. The other two will be described in Sections 3.3, 3.4.

3.2. Runge-Kutta CGC, direct discretization. The Fourier analysis of Gustafsson and Lötstedt [16, 26] only provides information on the phase speed of the smooth wave propagation. In this section, we extend the phase velocity analysis to include also the first correction term in the asymptotic expansions.

Suppose the coarse grid solve is carried out by one step of m-stage Runge-Kutta smoothing with coarse time step Δt_H, coarse mesh size H and the same CFL number λ as in the fine grid. The coarse grid correction matrix is then given by [16]:

$$C = I + \sum_{j=1}^{m} \Delta t_H^j \, p \, (L^H)^{j-1} \prod_{k=m-j+1}^{m} (-\alpha_k) r L^h.$$

In particular, for $m = 1$, $\Delta t_H = \lambda H$, we have

$$C = I - \lambda H p r L^h,$$

where p and r are the prolongation and restriction operators respectively. Let p be the linear interpolation and $r = \frac{1}{2}p^T$ its transpose. Then the Fourier transform of p is block diagonal with each diagonal subblock, $\hat{p}_\mu$, corresponding to Fourier frequency μ given by [18]:

$$\hat{p}_\mu = \frac{1}{\sqrt{2}} \begin{bmatrix} \cos(\mu\pi h) + 1 \\ \cos(\mu\pi h) - 1 \end{bmatrix} = \sqrt{2} \begin{bmatrix} c_\mu^2 \\ -s_\mu^2 \end{bmatrix}, \qquad \mu = 0, 1, \ldots, N-1,$$

where $c_\mu = \cos(\frac{\mu\pi h}{2})$ and $s_\mu = \sin(\frac{\mu\pi h}{2})$. Similarly, $\hat{r} = \frac{1}{2}\hat{p}^T$ is block diagonal with each subblock $\hat{r}_\mu = \frac{1}{2}\hat{p}_\mu^T$. Hence, the 2×2 subblocks of the Fourier transform of C are given by

$$\begin{aligned} \hat{C}_\mu &= I - \lambda H \hat{p}_\mu \hat{r}_\mu \hat{L}_\mu^h \\ &= I - \lambda H \begin{bmatrix} c_\mu^2 \\ -s_\mu^2 \end{bmatrix} \begin{bmatrix} c_\mu^2 & -s_\mu^2 \end{bmatrix} \frac{1}{h} \begin{bmatrix} 1 - e^{-\mu\pi h i} & 0 \\ 0 & 1 + e^{-\mu\pi h i} \end{bmatrix}. \end{aligned} \tag{9}$$

Since $\hat{M} = \hat{C}\hat{S}$, the study of $\hat{C}$ and hence $\hat{C}_\mu$ is crucial to the understanding of $\hat{M}$. We first have the following result by direct calculation.

LEMMA 3.1. *The eigenvalues of $\hat{C}_\mu$ are:*

$$\lambda_1 = 1, \quad \lambda_2 = 1 - 2\lambda c_\mu^4(1 - e^{-\mu\pi hi}) - 2\lambda s_\mu^4(1 + e^{-\mu\pi hi}).$$

Thus, the largest eigenvalue of $\hat{C}$ is equal to 1. Hence, in general, there maybe no error reduction. However, in the context of multigrid, the errors have been smoothed by the smoothing process. Thus, instead of considering the largest eigenvalues of $\hat{C}_\mu$, we are more interested in the low-low interaction, i.e. how the smooth waves are changed by the coarse grid correction. Hence, we focus just on the (1,1) entry of $\hat{C}_\mu$. By (9),

$$\begin{aligned} \hat{C}_\mu(1,1) &= 1 - 2\lambda c_\mu^4(1 - e^{-\mu\pi hi}) \\ &\equiv |\hat{C}_\mu(1,1)| e^{-i\kappa(\mu)\mu\pi h\lambda}. \end{aligned}$$

We note that in [16, 26], they considered the spectral radius of the iteration matrix, $\hat{M}$, and computed the leading order term of the asymptotic expansion of it. For higher order terms, we find that the formulae are too complicated to be illustrative. As as shown by the numerical results, it turns out that the convergence behavior can be determined quite accurately by the dissipation and phase velocity properties of C_{11}.

Here comes our result on the dispersion of $\hat{C}_\mu(1,1)$ which is not considered explicitly by Gustafsson and Lötstedt [16].

THEOREM 3.2. *The coarse grid correction is dissipative of order 2 for $0 < \lambda \le 1/2$, and dispersive. More precisely, the dissipation and phase velocity of $\hat{C}_\mu$ are given, respectively, by*

$$\begin{aligned} |\hat{C}_\mu(1,1)| &\le 1 \qquad \textit{if and only if} \qquad 0 < \lambda \le \frac{1}{2}, \\ \kappa(\mu) &= 2 + \frac{8\lambda - 15}{12}(\mu\pi h)^2 + O(\mu\pi h)^4. \end{aligned}$$

Proof.

$$\begin{aligned} \hat{C}_\mu(1,1) &= 1 - 2\lambda c_\mu^4(1 - e^{-\mu\pi hi}) \\ &= 1 - 2\lambda c_\mu^4 + 2\lambda c_\mu^4(\cos(\mu\pi h) - i\sin(\mu\pi h)) \\ &= [1 - \lambda c_\mu^2 \sin^2(\mu\pi h)] - i[2\lambda c_\mu^4 \sin(\mu\pi h)]. \end{aligned}$$

Thus the absolute value of $\hat{C}_\mu(1,1)$ is calculated as

$$\begin{aligned} |\hat{C}_\mu(1,1)|^2 &= [1 - \lambda c_\mu^2 \sin^2(\mu\pi h)]^2 + [2\lambda c_\mu^4 \sin(\mu\pi h)]^2 \\ &= 1 - 2\lambda c_\mu^2 \sin^2(\mu\pi h) + 4\lambda^2 c_\mu^6 \sin^2(\mu\pi h). \end{aligned}$$

Then $|\hat{C}_\mu(1,1)| \le 1$ if and only if

$$\begin{aligned} -2\lambda c_\mu^2 \sin^2(\mu\pi h) + 4\lambda^2 c_\mu^6 \sin^2(\mu\pi h) &\le 0 \\ \Rightarrow \qquad \lambda &\le \frac{1}{2}. \end{aligned}$$

By considering the phase angle of $\hat{C}_\mu(1,1)$, we have

$$\tan(\theta) = \frac{2\lambda c_\mu^4 \sin(\mu\pi h)}{1 - \lambda c_\mu^2 \sin^2(\mu\pi h)} = \frac{4\lambda c_\mu^5 s_\mu}{1 - 4\lambda c_\mu^4 s_\mu^2}.$$

Let $\xi = \mu\pi h$. By Taylor expansion of c_μ and s_μ,

$$\begin{aligned} \tan(\theta) &= \frac{4\lambda(1 - \frac{\xi^2}{8})^5(\frac{\xi}{2}) + O(\xi^3)}{1 - 4\lambda(1 - \frac{\xi^2}{8})^4(\frac{\xi}{2})^2 + O(\xi^4)} \\ &= 2\lambda\xi + (2\lambda^2 - \frac{5\lambda}{4})\xi^3 + O(\xi^5). \end{aligned}$$

By applying the Taylor expansion of arctan, we have

$$\begin{aligned}\theta(\mu) &= (2\lambda\xi + (2\lambda^2 - \frac{5\lambda}{4})\xi^3)(1 - \frac{1}{3}(2\lambda\xi)^2) + O(\xi^5) \\ &= 2\lambda\xi + (\frac{2\lambda^2}{3} - \frac{5\lambda}{4})\xi^3 + O(\xi^5).\end{aligned}$$

Hence, the phase velocity is given by

$$\kappa(\mu) = 2 + (\frac{2\lambda}{3} - \frac{5}{4})\xi^2 + O(\xi^4).$$

□

There are two implications of Theorem 3.2. First, considering $|\hat{C}_\mu(1,1)|$, the CFL condition on λ ($\leq \frac{1}{2}$) is more restrictive than that imposed by the Euler's smoothing ($\lambda \leq 1$). Secondly, the leading order term shows that the coarse grid correction has an effect of propagating smooth waves with speed 2. Furthermore, we note that the second term is negative for $0 < \lambda < 1$. Thus, the nonconstant smooth waves will have a negative phase velocity error, i.e. these modes are propagated slower, which accounts for the oscillations generated at the tail as the wave propagates to the right; see Figure 1.

Based on the phase velocity analysis, convergence will be delayed by oscillations unless the the smoother used is extremely effective in damping most of the high frequency Fourier modes, for instance, by the use of artificial viscosity, or modified Runge-Kutta methods. Another approach is to use a different interpolation, for instance, piecewise constant interpolation, motivated by the fact that the model PDE is first order. However, we note that the resulting multigrid is still dispersive (by a similar analysis as in Theorem 3.2). Hence, a fundamental change in the algorithm is needed to obtain a nonoscillatory multigrid method. Recently, Jameson and Wan proposed multigrid methods for linear and nonlinear wave equation in one dimension which are total variation diminishing and preserve monotonicity [23], and thus no dispersion.

3.3. Exact CGC, direct discretization. The dispersion effect discussed in Section 3.2 is largely due to the inexact coarse grid solve, and it explains that different waves travel at different speeds which delay the overall multigrid convergence. In this section, we consider exact coarse grid solve instead. Thus, as in standard multigrid, the idea is to eliminate the smooth errors completely on the coarse grid while the oscillatory errors are damped by the smoother. The coarse grid operators used are the same as before; we apply the same discretization scheme to all the coarse grids. An advantage of using the discretization matrices as the coarse grid operators is that the smoothing property on the fine grid will be also valid on all the subsequent coarse grids. Also, it saves storage since the coarse grid operators need not be stored. Linear interpolation is used for intergrid transfer. As an example, we apply this multigrid with 3 coarse grids to solve our model problem. The numerical solutions obtained are shown in Figure 2. Although the numerical solutions are converging to 0 (note the change in scale on the y-axis), the formation of the relatively large error in the middle is unexpected since the starting solution is very smooth, and the exact coarse grid solve should, in principle, have eliminated it completely.

We now discuss this numerical oscillation with the help of several plots, followed by a phase velocity analysis. We use the same multigrid method to solve the model problem. This time, we use 3 grids, and many smoothing steps (25, and $\lambda = 0.8$) to provide a better illustration. In Figure 3(a), we start with a smooth starting function $u^{(1)}$ (solid line) on the first grid, and obtain $\bar{u}^{(1)}$ (dashed line) after 25 smoothing steps. We then restrict the residual to the second grid and apply the two-grid method to solve the error equation on this grid. The initial guess is zero. The initial error, $e^{(2)}$, (solid line) and the error after 25 smoothing steps, $\bar{e}^{(2)}$, (dashed line) are shown in Figure 3(b). We then restrict the residual to the third grid and solve the error equation exactly. The coarse grid error is then interpolated back to the second grid as $pe^{(3)}$, (dotted line) in Figure 3(b). In principle, the coarse grid error $pe^{(3)}$ should approximate well the error on the current grid $\bar{e}^{(2)}$, which seems to be close, but it is clearly shifted a bit to the left. Thus, after the coarse grid correction, the error of the updated solution (dash-dotted line) shows an oscillation underneath $\bar{e}^{(2)}$ due to the shift. Finally, we interpolate the solution on the second grid, which is the coarse grid error for the first grid, back to the first grid. The

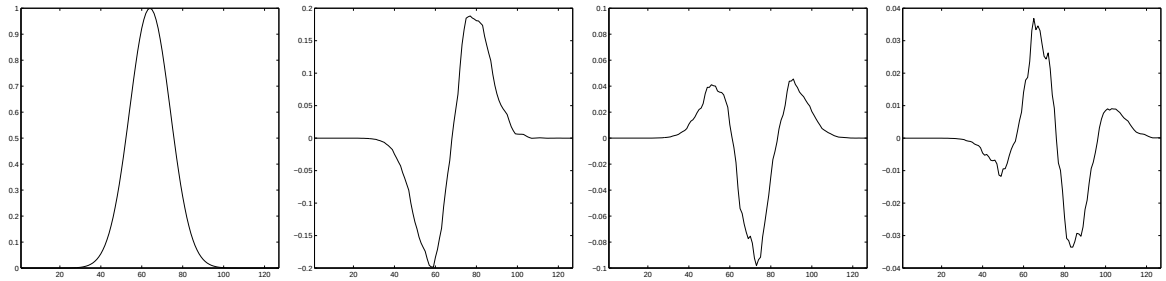

FIG. 2. *The numerical solutions given by a 4-level multigrid with exact coarse grid solve at (a) iteration = 0, (b) iteration = 1, (c) iteration = 2, (d) iteration = 3.*

solution after the coarse grid correction (dash-dotted) is shown in Figure 3(c). Instead of obtaining a near zero function, we have two oscillations corresponding to the coarse grid corrections of the second and third grids, respectively.

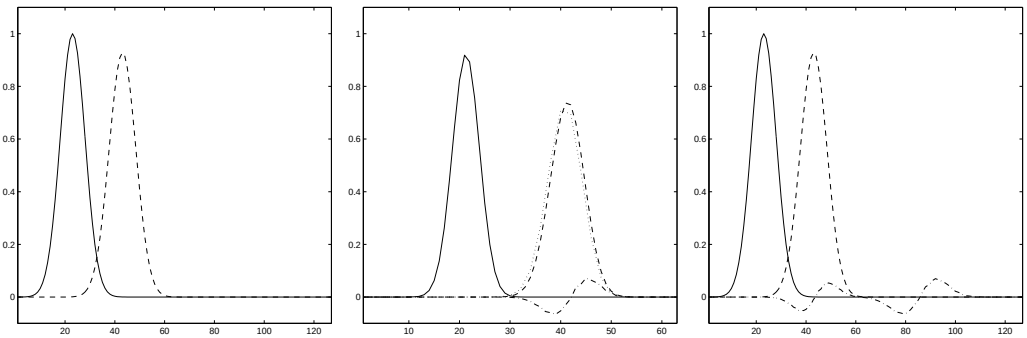

FIG. 3. *The initial error (solid line), error after smoothing (dashed line), error from coarse grid correction (dotted line), error after coarse grid correction (dash-dotted line) on (a) first grid, (b) second grid, (c) first grid.*

Thus, the oscillations occur immediately after the coarse grid correction and it is due to the difference in the phase velocity on the coarse grid. We use a phase velocity analysis to explain this phenomenon for the two-grid method. With exact coarse grid solve, the coarse grid correction matrix is:

$$C = I - p(L^H)^{-1} r L^h.$$

As in the previous approach, we are interested in the low-low interaction, i.e. the (1,1) entry of $\hat{C}_\mu$.

THEOREM 3.3. *The coarse grid correction of smooth waves given by the exact coarse grid solve together with linear interpolation is only first order accurate, with*

$$|\hat{C}_\mu(1,1)| = \frac{\mu\pi h}{2} + O(\mu\pi h)^2.$$

Proof. We separate the analysis of C into two steps. We first consider the term $D \equiv p(L^H)^{-1} r L^h$; i.e. the effect of exact coarse grid solve. The Fourier transformed coarse grid solve matrix D is given by

$$\begin{aligned}
\hat{D}_\mu &= \hat{p}_\mu (\hat{L}^H_\mu)^{-1} \hat{r}_\mu \hat{L}^h \\
&= \begin{bmatrix} c_\mu^2 \\ -s_\mu^2 \end{bmatrix} \frac{2h}{1 - e^{-2\mu\pi hi}} \begin{bmatrix} c_\mu^2 & -s_\mu^2 \end{bmatrix} \frac{1}{h} \begin{bmatrix} 1 - e^{-\mu\pi hi} & 0 \\ 0 & 1 + e^{-\mu\pi hi} \end{bmatrix} \\
&= 2 \begin{bmatrix} c_\mu^4 & -s_\mu^2 c_\mu^2 \\ -s_\mu^2 c_\mu^2 & s_\mu^4 \end{bmatrix} \begin{bmatrix} \frac{1}{1+e^{-\mu\pi hi}} & 0 \\ 0 & \frac{1}{1-e^{-\mu\pi hi}} \end{bmatrix}.
\end{aligned}$$

Hence, the (1,1) entry of $\hat{D}_\mu$ is

$$\hat{D}_\mu(1,1) = \frac{2c_\mu^4}{1+e^{-\mu\pi hi}} = c_\mu^4 + is_\mu c_\mu^3 = c_\mu^3 e^{\mu\pi hi/2}.$$

As a result,

$$\hat{C}_\mu(1,1) = 1 - \hat{D}_\mu(1,1) = 1 - c_\mu^3 e^{\mu\pi hi/2}.$$

The amplification factor can be easily calculated as

$$|\hat{C}_\mu(1,1)|^2 = (1-c_\mu^4)^2 + s_\mu^2 c_\mu^6,$$

and by Taylor expansion, we have the estimate

$$|\hat{C}_\mu(1,1)| = \frac{\mu\pi h}{2} + O(\mu\pi h)^2.$$

□

Comparing the formula of $\hat{D}_\mu(1,1)$ and Euler's smoothing, we can see that $\hat{D}_\mu(1,1)$ has the effect of shifting waves of any frequency by 1/2 grid point (to the left) immediately after the exact coarse grid solve. In other words, the coarse grid error given by the exact coarse grid solve and the fine grid error differ by 1/2 grid point. Thus, it explains precisely the slight shift of the coarse grid correction error (dash-dotted line) shown in Figure 3(b). As we shall see in the next section, this shift arises essentially from the discretization of the first order PDE with two different mesh sizes which cause dispersion to occur.

Due to the shift generated by $\hat{D}_\mu(1,1)$, the amplification factor of $\hat{C}_\mu(1,1) = O(\mu\pi h)$, i.e. the coarse grid correction is only first order accurate, instead of the second order accuracy one expects from linear interpolation.

We remark that in contrast to the Runge-Kutta CGC approach in Section 3.2, the exact coarse grid correction has no further restriction on the stability condition. Also, by Theorem 3.3, the oscillation generated by the coarse grid correction has a magnitude of $O(h)$. Finally, in this case, we do not consider the phase velocity of the coarse grid correction since the wave propagation concept on the coarse grid is not well-defined when exact coarse grid solve is used.

3.4. Galerkin CGC. In the elliptic case, one often uses Galerkin approach to form the coarse grid correction operator

$$G^H = rL^h p,$$

since the coarse grid error is minimized in the A-norm. For hyperbolic equations, however, the Galerkin coarse grid operator is less commonly used. In this section, we consider the use of Galerkin coarse grid operator with exact coarse grid solve and show that it does not have the dispersion effect caused by the discretization matrix on the coarse grid as in the non-Galerkin approach. We note that in [16], the Galerkin coarse grid operator is found to be unstable with centered finite differencing on the fine grid. However, we found it to be stable when upwinding is used on the fine grid.

We start with a similar numerical experiment as in the previous section. This time, we only use two grids. In Figure 4(a), it shows the smooth starting function and the solution after 25 smoothing steps. An exact coarse grid solve is used where the coarse grid operator is formed by Galerkin. The interpolated coarse grid error (dotted line) and the error after coarse grid correction (dash-dotted line) are shown in Figure 4(b). We see that the coarse grid error approximate well the error on the fine grid, and hence the error after the coarse grid correction is essentially gone; thus, there is no visible oscillation.

We explain the numerical observation by the phase angle analysis. Since the coarse grid operator is obtained by the Galerkin process, its Fourier transform can be calculated as follows:

$$\begin{aligned}\hat{G}_\mu^H &= \hat{r}_\mu \hat{A}_\mu^h \hat{p}_\mu \\ &= \begin{bmatrix} c_\mu^2 & -s_\mu^2 \end{bmatrix} \begin{bmatrix} 1-e^{-\mu\pi hi} & 0 \\ 0 & 1+e^{-\mu\pi hi} \end{bmatrix} \begin{bmatrix} c_\mu^2 \\ -s_\mu^2 \end{bmatrix}.\end{aligned}$$

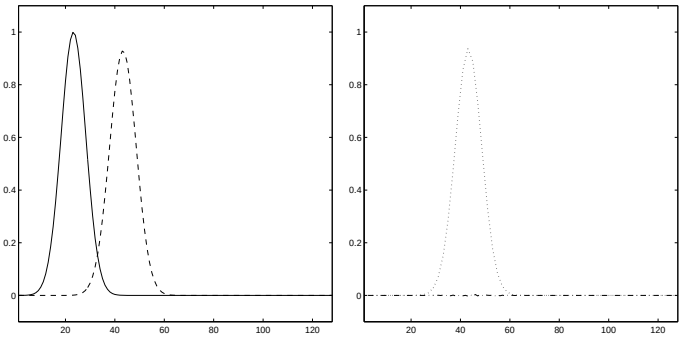

FIG. 4. *(a) The initial error (solid line) and error after smoothing (dashed line), (b) The error from coarse grid correction (dotted line) and error after coarse grid correction (dash-dotted line) on the first grid.*

After simplification, we have

$$\hat{G}_\mu^H = \frac{\cos^2(\mu\pi h) - e^{-2\mu\pi hi}}{2h}.$$

THEOREM 3.4. *The coarse grid correction of smooth waves given by the exact coarse grid solve together with Galerkin coarse grid operator is third order accurate, with*

$$|\hat{C}_\mu(1,1)| = \frac{1}{8}(\mu\pi h)^3 + O(\mu\pi h)^5.$$

Proof. We consider first the Fourier transform of the coarse grid solve matrix, D:

$$\begin{aligned}\hat{D}_\mu &= \hat{p}_\mu(\hat{L}_\mu^H)^{-1}\hat{r}_\mu\hat{L}_\mu^h \\ &= \begin{bmatrix} c_\mu^2 \\ -s_\mu^2 \end{bmatrix} \frac{2h}{\cos^2(\mu\pi h) - e^{-2\mu\pi hi}} \begin{bmatrix} c_\mu^2 & -s_\mu^2 \end{bmatrix} \frac{1}{h} \begin{bmatrix} 1 - e^{-\mu\pi hi} & 0 \\ 0 & 1 + e^{-\mu\pi hi} \end{bmatrix}.\end{aligned}$$

Thus the (1,1) entry of $\hat{D}_\mu$ is

$$\hat{D}_\mu(1,1) = \frac{2c_\mu^4(1 - e^{-\mu\pi hi})}{\cos^2(\mu\pi h) - e^{-2\mu\pi hi}} = \frac{c_\mu^3}{c_\mu^6 + s_\mu^6}(c_\mu^3 + is_\mu^3).$$

By direct calculation, the amplification factor of $\hat{D}_\mu(1,1)$ is

$$|\hat{D}_\mu(1,1)| = \frac{c_\mu^3}{\sqrt{c_\mu^6 + s_\mu^6}}.$$

Thus, dissipation is small for $\mu \approx 0$, which is necessary for an effective coarse grid correction. A more important issue is dispersion. The phase angle θ of $\hat{D}_\mu(1,1)$ is given by

$$\theta(\mu\pi h) = \arctan(\frac{s_\mu^3}{c_\mu^3}) = \frac{1}{8}(\mu\pi h)^3 + O(\mu\pi h)^5.$$

Now, we consider the Fourier transform of the coarse grid correction matrix, $\hat{C}$, in particular, its (1,1) entry:

$$\begin{aligned}\hat{C}_\mu(1,1) &= 1 - \hat{D}_\mu(1,1) \\ &= \frac{s_\mu^3}{c_\mu^6 + s_\mu^6}(s_\mu^3 - ic_\mu^3).\end{aligned}$$

By Taylor expansion, we have

$$\begin{aligned} |\hat{C}_\mu(1,1)| &= \frac{s_\mu^3}{\sqrt{c_\mu^6 + s_\mu^6}} \\ &= \frac{1}{8}(\mu\pi h)^3 + O(\mu\pi h)^5. \end{aligned}$$

□

First, we see that the phase angle of $\hat{D}_\mu(1,1)$ in the Galerkin approach is two orders of magnitude smaller than that in the non-Galerkin approach, implying that essentially no shifting occurs after the exact coarse grid solve. Consequently, the coarse grid correction operator is 2 orders more accurate.

4. Two dimensions. We extend the phase velocity analysis of Section 3.2 to two dimensions. Consider the convection dominated problem on a unit square:

$$-\epsilon\Delta u + a(x,y)u_x + b(x,y)u_y = f \qquad x \in \Omega = (-1,1)\times(-1,1),$$

with periodic boundary condition. In particular, we focus on two model problems:

(1) Entering flow (constant coefficient):

$$a(x,y) \equiv a, \quad b(x,y) \equiv b.$$

(2) Recirculating flow (variable coefficient):

$$a(x,y) = 4x(x-1)(1-2y), \quad b(x,y) = -4y(y-1)(1-2x).$$

We discretize the equation using the first order upwind scheme on a uniform fine grid $\{(x_j^h, y_k^h)\}_{-N\le j,k\le N-1}$ with mesh size h, resulting in a linear system

$$L^h u^h = f^h,$$

where

$$\begin{aligned} (L^h u^h)_{i,j} &= \epsilon\frac{4u_{i,j}^h - u_{i-1,j}^h - u_{i+1,j}^h - u_{i,j-1}^h - u_{i,j+1}^h}{h^2} \\ &\quad + \frac{(-a-|a|)u_{i-1,j}^h + 2|a|u_{i,j}^h + (a-|a|)u_{i+1,j}^h}{2h} \\ &\quad + \frac{(-b-|b|)u_{i,j-1}^h + 2|b|u_{i,j}^h + (b-|b|)u_{i,j+1}^h}{2h}; \end{aligned}$$

see, for instance, [12]. Since our primary focus is on the limit $\epsilon \to 0$, we shall ignore the elliptic term in the analysis. As in the one-dimensional case, we are interested in the convergence of the iteration error.

We remark that Gauss-Seidel smoothing with "downstream ordering" is often used in multigrid for convection-dominated problems [1, 10, 19, 25, 33]. In this approach, the role of Gauss-Seidel is not only a smoother but also, at least in part, as a solver. In this paper, however, we only concentrate on the effect of coarse grid correction, and hence we do not take into account the ordering issue.

Denote the two-dimensional discrete Fourier functions by $\psi_{\mu,\nu}^h$ where

$$\psi_{\mu,\nu}^h(x_{j,k}^h) = \frac{1}{2}e^{i\mu\pi x_j^h}e^{i\nu\pi y_k^h} \qquad -N \le \mu,\nu \le N-1,$$

which form an orthonormal basis with respect to the usual discrete l_2 inner product. The functions $\psi_{\mu,\nu}^h$, with $|\mu|, |\nu| \approx 0$, correspond to low frequency modes where $\psi_{\mu,\nu}^h$, with $|\mu|, |\nu| \approx N$, correspond to high frequency modes. In two dimension, we also have mixed low-high and high-low modes.

As in one dimension, we group corresponding low-low, high-low, low-high, and high-high modes together as:

$$Q_h = [\cdots \psi^h_{\mu,\nu}\ \psi^h_{\mu,\nu'}\ \psi^h_{\mu',\nu}\ \psi_{\mu',\nu'} \cdots],$$

where $\mu' = \mu - N$, $\nu' = \nu - N$. We state the standard Fourier results as follows [18, 34].

LEMMA 4.1. *Let $\hat{L}^h$, $\hat{p}^h$ and $\hat{r}^h$ be the Fourier transform matrices of L^h, p^h and r^h, respectively. Then $\hat{L}^h$ is block diagonal with 4×4 subblocks $\hat{L}^h_{\mu,\nu}$. $\hat{p}^h$ is block diagonal with 4×1 subblocks $\hat{p}^h_{\mu,\nu}$. $\hat{r}^h$ is block diagonal with 1×4 subblocks $\hat{r}^h_{\mu,\nu}$.*

For the entering flow problem, the 2×2 subblocks of the Fourier transform discretization matrix is given by

$$\hat{L}^h_{\mu,\nu} = \frac{a}{h}(1 - e^{-\mu\pi hi}) + \frac{b}{h}(1 - e^{-\nu\pi hi}).$$

Suppose the first order Runge-Kutta smoother is used. The Fourier transform of the iteration matrix is given by:

$$\begin{aligned} \hat{S}^h_{\mu,\nu} &= 1 - \Delta t \hat{L}^h_{\mu,\nu} \\ &= 1 - a\lambda(1 - e^{-\mu\pi hi}) - b\lambda(1 - e^{-\nu\pi hi}). \end{aligned} \tag{10}$$

Unfortunately, even for this constant coefficient case, the formula (after simplification) given by (10) does not provide much insight into the qualitative behavior of $\hat{S}_{\mu,\nu}$. We demonstrate the propagation behavior of the smoother by a numerical experiment. We take $a = b = 1$ and the CFL number $\lambda = 0.4$. The mesh size is $h = 1/16$. The plots of the spectrum of $\hat{S}^h$ are shown in Figure 5(a) and (b). For the 2D constant coefficient case, we define the phase velocity to be:

$$\kappa(\mu, \nu) = \frac{arg(\hat{S}_{\mu,\nu})}{\Delta t_h \pi(a\mu + b\nu)}.$$

Figure 5(a) shows that dissipation is small for low frequencies ($\mu, \nu \approx 0$), and around 0.6 near the high frequencies. It is interesting to notice that the frequencies corresponding to the largest dissipation is in the middle of the spectrum. Figure 5(b) shows that the phase velocity of low frequencies is about 1, which is consistent with the differential equation.

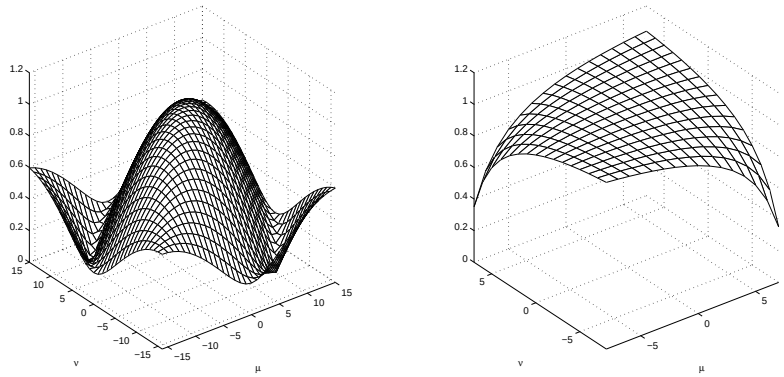

FIG. 5. *Spectrum of the Fourier transform of Euler's smoother for the entering flow problem. (a) $|\hat{S}^h_{\mu,\nu}|$, (b) Phase velocity of $\hat{S}^h_{\mu,\nu}$ (only the low frequencies are shown).*

4.1. Runge-Kutta CGC, direct discretization. In the one-dimensional analysis, we conclude that the multigrid V-cycle convergence is delayed by the oscillation generated as a result of the dispersive effect caused by the coarse grid correction. In the following, we shall show that similar oscillations occur also in the two-dimensional case. As in 1D, we start with the wave propagation

approach, i.e. the coarse grid solve is done by a few smoothing steps. The interpolation, p, and the restriction, r, is bilinear and full weighting, respectively; hence $r = 1/4p^T$. The smoother is the same as in one dimension – first Euler's method, which is also Richardson smoothing.

Assuming a ,b constant, the Fourier transform of the coarse grid correction matrix C is given by

$$\begin{aligned}\hat{C}_{\mu,\nu} &= I - \lambda H \hat{p}_{\mu,\nu}\hat{r}_{\mu,\nu}\hat{L}^h_{\mu,\nu} \\ &= I - 2\lambda h \begin{bmatrix} c_\mu^2 c_\nu^2 \\ -s_\mu^2 c_\nu^2 \\ -c_\mu^2 s_\nu^2 \\ s_\mu^2 s_\nu^2 \end{bmatrix} \begin{bmatrix} c_\mu^2 c_\nu^2 & -s_\mu^2 c_\nu^2 & -c\mu^2 s_\nu^2 & s_\mu^2 s_\nu^2 \end{bmatrix} \hat{L}^h_{\mu,\nu}.\end{aligned}$$

In particular, we are interested in the (1,1) entry of $\hat{C}_{\mu,\nu}$,

$$\hat{C}_{\mu,\nu}(1,1) = 1 - 2\lambda h c_\mu^4 c_\nu^4 [\frac{a}{h}(1 - e^{-\mu\pi hi}) + \frac{b}{h}(1 - e^{-\nu\pi hi})].$$

To get more insight into the formula of $\hat{C}_{\mu,\nu}(1,1)$, we consider the special case where $a = b = 1$ and frequencies in the characteristic direction, i.e. $\nu = \mu$.

THEOREM 4.2. *Assume $a = b = 1$. In the characteristic direction, i.e. $\nu = \mu$, the coarse grid correction is dissipative for $0 < \lambda \leq 1/4$, and dispersive, i.e.*

$$\begin{aligned}|\hat{C}_\mu(1,1)| &\leq 1 \qquad \textit{if and only if} \qquad 0 < \lambda \leq \frac{1}{4}, \\ \kappa(\mu) &= 2 + (2\lambda - \frac{9}{4})(\mu\pi h)^2 + O(\mu\pi h)^4.\end{aligned}$$

Proof. Under the assumptions,

$$\begin{aligned}\hat{C}_{\mu,\nu}(1,1) &= 1 - 2\lambda h c_\mu^8 [\frac{2}{h}(1 - e^{-\mu\pi hi})] \\ &= 1 - 2\lambda c_\mu^6 \sin^2(\mu\pi h) - i4\lambda c_\mu^8 \sin(\mu\pi h).\end{aligned}$$

The desired results follow from a similar calculation as in the proof of Theorem 3.2. □

Figure 6(a) shows $\max_{\mu,\nu} |\hat{C}_{\mu,\nu}(1,1)|$ for different values of λ, $a = b = 1$. We note that the stability requirement for the coarse grid correction is $0 \leq \lambda \leq 1/4$ whereas that for smoothing is only $0 \leq \lambda \leq 1/2$. Thus, a more restrictive CFL number is needed, which is consistent with the one-dimensional result (cf. Theorem 3.2). For $\lambda = 0.25$, Figure 6(b) shows that $\hat{C}_{\mu,\nu}(1,1)$ is dissipative for all values of μ, ν. Figure 6(c) shows the phase velocity of $\hat{C}_{\mu,\nu}(1,1)$. For $\mu, \nu \approx 0$, the phase velocity is approximately 2; thus smooth waves propagate at a speed of 2 on the coarse grid. Moreover, as μ, ν increases, the phase velocity decreases from 2, suggesting that dispersion also occurs in the 2D case.

As an example, we solve the model entering flow problem by multigrid, and snap shots of the errors in the first 15 V-cycles are shown in Figure 7. We use bilinear interpolation, one pre-smoothing, and 3 grids. The mesh size is $h = 1/32$, and $\lambda = 0.25$. We observe that oscillations are generated at the tail as the square wave propagates from (-1,-1) to (1,1), which agrees with our phase velocity analysis.

For the recirculating flow problem, Fourier analysis is not feasible, and yet we still observe a similar wave propagation phenomenon as in the entering flow problem; see Figure 8. The same parameters are used as for the entering flow problem. We can see that the wave rotates around the domain with oscillations at the tail generated by the dispersion of the coarse grid correction. Thus, the results of the phase velocity analysis for constant coefficient problems appear to hold also for variable coefficient problems.

4.2. Exact CGC, direct discretization. Instead of applying a few steps of smoothing on the coarse grid, we solve the coarse grid equation exactly. Direct discretization is used for the coarse grid operator. Thus, the coarse grid correction matrix is

$$C = I - p(L^H)^{-1} r L^h,$$

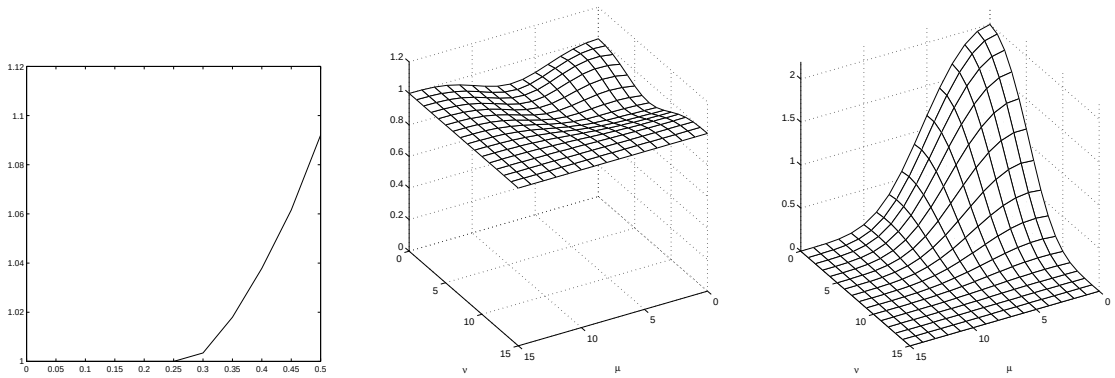

FIG. 6. *Spectrum of the Fourier transform of the inexact coarse grid correction for the entering flow problem. (a)* $\max_{\mu,\nu} |\hat{C}_{\mu,\nu}(1,1)|$ *with CFL number* $0 \leq \lambda \leq 0.5$*, (b)* $|\hat{C}_{\mu,\nu}(1,1)|$*,* $\lambda = 0.25$*, (c) Phase velocity of* $\hat{C}_{\mu,\nu}(1,1)$*.*

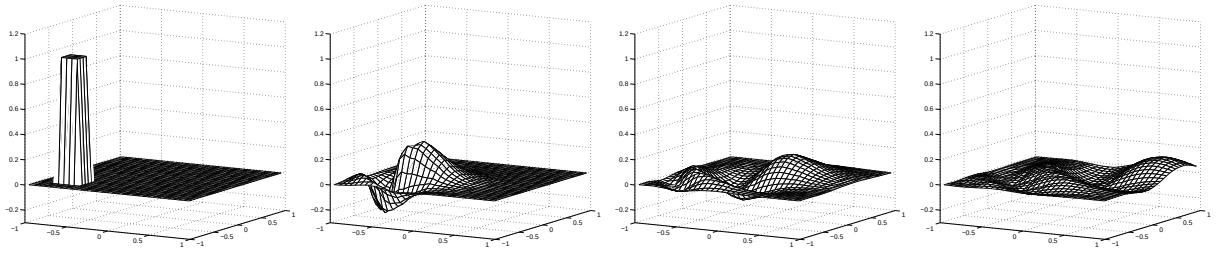

FIG. 7. *Numerical solutions given by a 3-level multigrid for the entering flow problem at (a) iteration = 0, (b) iteration = 5, (c) iteration = 10, (d) iteration = 15.*

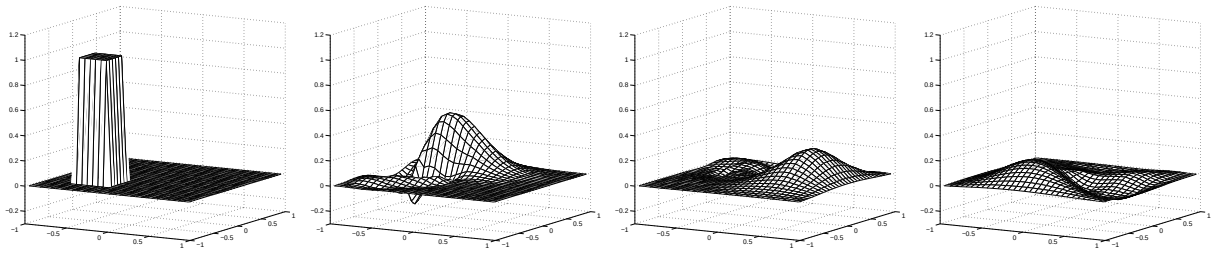

FIG. 8. *Numerical solutions given by a 3-level multigrid for the recirculating flow problem at (a) iteration = 0, (b) iteration = 5, (c) iteration = 10, (d) iteration = 15.*

and its Fourier transform is given by

$$\begin{aligned}\hat{C}_{\mu,\nu} &= I - \hat{p}_{\mu,\nu}(\hat{L}^H_{\mu,\nu})^{-1}\hat{r}_{\mu,\nu}\hat{L}^h_{\mu,\nu} \\ &= I - \begin{bmatrix} c_\mu^2 c_\nu^2 \\ -s_\mu^2 c_\nu^2 \\ -c_\mu^2 s_\nu^2 \\ s_\mu^2 s_\nu^2 \end{bmatrix} \frac{1}{\frac{a}{2h}(1-e^{-\mu\pi 2hi}) + \frac{b}{2h}(1-e^{-\nu\pi 2hi})} \begin{bmatrix} c_\mu^2 c_\nu^2 & -s_\mu^2 c_\nu^2 & -c\mu^2 s_\nu^2 & s_\mu^2 s_\nu^2 \end{bmatrix} \hat{L}^h_{\mu,\nu}.\end{aligned}$$

Therefore,

$$\hat{C}_{\mu,\nu}(1,1) = 1 - c_\mu^4 c_\nu^4 \frac{\frac{a}{h}(1-e^{-\mu\pi hi}) + \frac{b}{h}(1-e^{-\nu\pi hi})}{\frac{a}{2h}(1-e^{-\mu\pi 2hi}) + \frac{b}{2h}(1-e^{-\nu\pi 2hi})}.$$

To better understand the formula of $\hat{C}_{\mu,\nu}(1,1)$, we consider two special and yet important cases: frequency components in the characteristic direction, i.e. (μ,ν) such that

$$b\mu - a\nu = 0,$$

and, cross-characteristic direction [3, 12, 38], i.e. (μ,ν) such that

$$a\mu + b\nu = 0.$$

THEOREM 4.3. *For the components in the characteristic direction and assuming $a = b$,*

$$|\hat{C}_{\mu,\nu}(1,1)| = \frac{\mu\pi h}{2} + O(\mu\pi h)^2.$$

For the components in the cross-characteristic direction and general a, b,

$$\lim_{\mu\to 0} \hat{C}_{\mu,\nu}(1,1) = \frac{1}{2}.$$

In particular, for $a = b$, then $\hat{C}_{\mu,\nu}(1,1) = 1 - c_\mu^6/2$.

Proof. As in the corresponding one-dimensional case, we are also interested in the effect of the exact coarse grid solve, i.e. $D = p(L^H)^{-1}rL^h$, whose Fourier transform is given by

$$\hat{D}_{\mu,\nu}(1,1) = c_\mu^4 c_\nu^4 \frac{\frac{a}{h}(1-e^{-\mu\pi hi}) + \frac{b}{h}(1-e^{-\nu\pi hi})}{\frac{a}{2h}(1-e^{-\mu\pi 2hi}) + \frac{b}{2h}(1-e^{-\nu\pi 2hi})}.$$

In the characteristic direction, and $a = b$, then

$$\hat{D}_{\mu,\nu}(1,1) = c_\mu^8 \frac{2a(1-e^{-\mu\pi hi})}{a(1-e^{-2\mu\pi hi})} = c_\mu^7 e^{\frac{\mu\pi hi}{2}}.$$

As a result,

$$\hat{C}_{\mu,\nu}(1,1) = 1 - c_\mu^7 e^{\frac{\mu\pi hi}{2}} = 1 - c_\mu^8 - is_\mu c_\mu^7.$$

Then, we have $|\hat{C}_{\mu,\nu}(1,1)|^2 = 1 - 2c_\mu^8 + c_\mu^{14}$, and hence

$$|\hat{C}_{\mu,\nu}(1,1)| = \frac{\mu\pi h}{2} + O(\mu\pi h)^2.$$

In the cross-characteristic direction, and general a, b, by l'Hospital's rule,

$$\begin{aligned}\lim_{\mu\to 0} \hat{C}_{\mu,\nu}(1,1) &= 1 - \lim_{\mu\to 0} \frac{2a(1-e^{-\mu\pi hi}) + 2b(1-e^{\frac{a}{b}\mu\pi hi})}{a(1-e^{-2\mu\pi hi}) + b(1-e^{2\frac{a}{b}\mu\pi hi})} \\ &= 1 - \lim_{\mu\to 0} \frac{2a(\pi hi)e^{-\mu\pi hi} - 2a(\pi hi)e^{\frac{a}{b}\mu\pi hi}}{2a(\pi hi)e^{-2\mu\pi hi} - 2a(\pi hi)e^{2\frac{a}{b}\mu\pi hi}} \\ &= 1 - \lim_{\mu\to 0} \frac{1}{e^{-\mu\pi hi} + e^{\frac{a}{b}\mu\pi hi}} \\ &= \frac{1}{2}.\end{aligned}$$

For $a = b = 1$, the explicit formula for $\hat{C}_{\mu,\nu}(1,1)$ follows from direct substitution. □

We note that our analysis for the cross-characteristic direction is consistent with the result of Brandt and Yavneh [12] in which they also showed that $\lim_{\mu\to 0} \hat{C}_{\mu,\nu}(1,1) = 1/2$ for the special case $b = 0$, and so they concluded that the coarse grid error is not a good approximation to the fine grid error for components in the cross-characteristic directions. In [38], Yavneh proposes the use of higher order interpolation and restriction operators and more accurate discretizations of the coarse grid operator to improve the accuracy of the coarse grid correction.

In both [12, 38], the phase error is not discussed which has been shown by Theorem 4.3 to be relevant for components in the characteristic direction. Specifically, in the characteristic direction, magnitude of these components is accurate: $|\hat{D}_{\mu,\nu}(1,1)| = c_\mu^7$, $\mu \approx 0$. However, it has a phase error of $\mu\pi h/2$. Qualitatively speaking, the coarse grid error is shifted by $h/2$ in the characteristic direction, and hence the accuracy of $\hat{C}_{\mu,\nu}(1,1)$ is only first order.

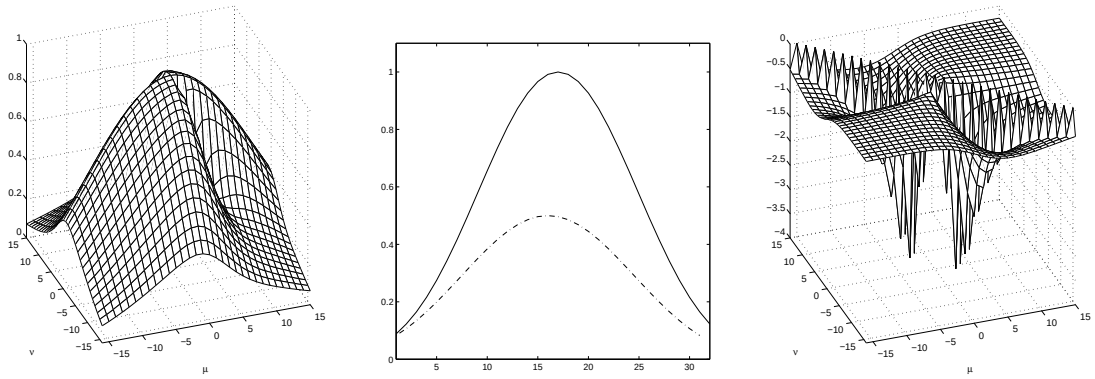

FIG. 9. *Spectrum of the Fourier transform of $D = p(L^H)^{-1} r L^h$ where L^H is obtained from the direct discretization of the entering flow problem. (a) $|\hat{D}_{\mu,\nu}(1,1)|$, (b) $|\hat{D}_{\mu,\nu}(1,1)|$, $\mu = \nu$ (solid line) and $\mu = -\nu$ (dashed line) (c) Scaled phase angle of $\hat{D}_{\mu,\nu}(1,1)$.*

Figure 9(a) shows that $|\hat{D}_{\mu,\nu}(1,1)| \approx 1$, for $\mu, \nu \approx 0$ and having the same sign, but significantly below 1 for other values of μ and ν. In Figure 9(b), we plot the values of $|\hat{D}_{\mu,\nu}(1,1)|$ for the case $\mu = \nu$ (solid line) and $\mu = -\nu$ (dashed line). Both agree with the results of Theorem 4.3. Figure 9(c) shows the scaled values of the phase angles, $\frac{\theta}{(\mu+\nu)\pi h}$, which measures the amount of shift in the coarse grid error along the flow direction. In the characteristic direction, the amount of shift is negative and relatively constant. In the cross-characteristic direction, the amount of shift varies. Thus, we expect the coarse grid error is slightly shifted from the fine grid error.

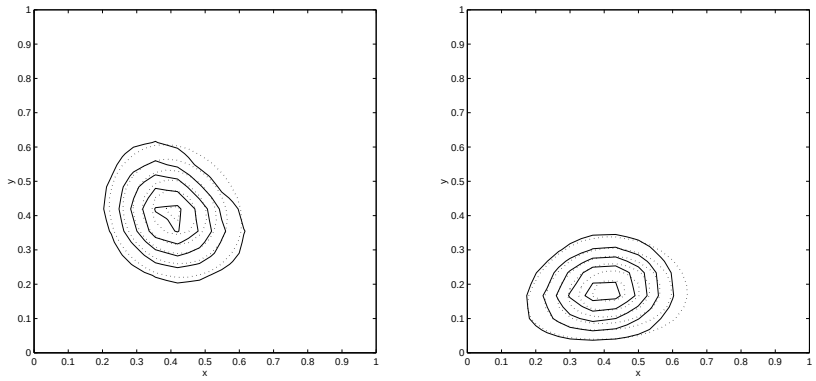

FIG. 10. *Contour plots of the fine grid error (dashed line) and the interpolated coarse grid error (solid line) for (a) the entering flow, and (b) the recirculating flow,.*

Figure 10(a) and (b) show the contour plots of the fine grid error (dashed line) and the interpolated coarse grid error (solid line) for the entering flow and recirculating flow, respectively. Both results agree with the phase analysis that the interpolated coarse grid errors are shifted behind the directions of the flow. We note that the amount of shift depends on the mesh size and hence it get more serious on the coarser mesh which occurs when many levels of multigrid are used.

4.3. Galerkin CGC. To avoid the shifting phenomenon, we use the Galerkin approach to form the coarse grid operator, i.e.

$$G^H = rL^h p.$$

Thus, the coarse grid correction matrix is given by

$$C = I - p(G^H)^{-1} r L^h,$$

and its Fourier transform is:

$$\begin{aligned} \hat{C}_{\mu,\nu} &= I - \hat{p}_{\mu,\nu}(\hat{G}^H_{\mu,\nu})^{-1}\hat{r}_{\mu,\nu}\hat{L}^h_{\mu,\nu} \\ &= I - \hat{p}_{\mu,\nu}(\hat{r}_{\mu,\nu}\hat{L}^h_{\mu,\nu}\hat{p}_{\mu,nu})^{-1}\hat{r}_{\mu,\nu}\hat{L}^h_{\mu,\nu}. \end{aligned}$$

We again consider the characteristic and cross-characteristic components.

THEOREM 4.4. *For the components in the characteristic direction and assuming constant $a = b$,*

$$|\hat{C}_{\mu,\nu}(1,1)| = \frac{(\mu\pi h)^3}{8} + O(\mu\pi h)^5.$$

For the components in the cross-characteristic direction and general a, b,

$$\lim_{\mu\to 0} \hat{C}_{\mu,\nu}(1,1) = 0.$$

In particular, if $a = b$, then

$$|\hat{C}_{\mu,\nu}(1,1)| = \frac{(\mu\pi h)^2}{4} + O(\mu\pi h)^4.$$

Proof. First, consider $D = p(G^H)^{-1} r L^h$. Fourier transform gives

$$\hat{D}_{\mu,\nu}(1,1) = c_\mu^4 c_\nu^4 \frac{\hat{L}^h_{\mu,\nu}}{\hat{G}^H_{\mu,\nu}}, \tag{11}$$

where the Fourier transform of the Galerkin coarse grid operator is given by

$$\begin{aligned} \hat{G}^H_{\mu,\nu} &= c_\mu^4 c_\nu^4 [\frac{a}{h}(1 - e^{-\mu\pi hi}) + \frac{b}{h}(1 - e^{-\nu\pi hi})] + s_\mu^4 c_\nu^4 [\frac{a}{h}(1 + e^{-\mu\pi hi}) + \frac{b}{h}(1 - e^{-\nu\pi hi})] \\ &\quad + c_\mu^4 s_\nu^4 [\frac{a}{h}(1 - e^{-\mu\pi hi}) + \frac{b}{h}(1 + e^{-\nu\pi hi})] + s_\mu^4 s_\nu^4 [\frac{a}{h}(1 + e^{-\mu\pi hi}) + \frac{b}{h}(1 + e^{-\nu\pi hi})]. \end{aligned}$$

In the characteristic direction and $a = b$, (11) becomes

$$\hat{D}_{\mu,\nu}(1,1) = \frac{c_\mu^7}{(c_\mu^4 + s_\mu^4)(c_\mu^6 + s_\mu^6)}(c_\mu^3 + i s_\mu^3).$$

Let $\hat{D}_{\mu,\nu}(1,1) = |\hat{D}_{\mu,\nu}(1,1)| e^{i\theta}$, and by direct calculation

$$\begin{aligned} |\hat{D}_{\mu,\nu}(1,1)| &= \frac{c_\mu^7}{(c_\mu^4 + s_\mu^4)\sqrt{c_\mu^6 + s_\mu^6}}, \\ \theta &= \frac{1}{8}(\mu\pi h)^3 + O(\mu\pi h)^5. \end{aligned}$$

Thus, the coarse grid error is accurate in magnitude and the phase shift is negligibly small. Moreover, we have

$$\begin{aligned}\hat{C}_{\mu,\nu}(1,1) &= 1-\hat{D}_{\mu,\nu}(1,1)\\ &= \frac{c_\mu^4 s_\mu^4 + s_\mu^{10} - i s_\mu^3 c_\mu^7}{(c_\mu^4+s_\mu^4)(c_\mu^6+s_\mu^6)},\end{aligned}$$

and Taylor expansion of which gives the result.

In the cross-characteristic directions, general a, b, we obtain the limit result by a similar calculation as in the proof of Theorem 4.3. Finally, if in addition, $a = b$, then

$$\begin{aligned}\hat{C}_{\mu,\nu}(1,1) &= 1-\frac{c_\mu^2 s_\mu^2 + s_\mu^6}{c_\mu^6 + c_\mu^2 s_\mu^2 + s_\mu^6}\\ &= \frac{(\mu\pi h)^2}{4} + O(\mu\pi h)^4.\end{aligned}$$

□

In the Galerkin approach, the magnitudes of smooth coarse grid errors are 1 for both cross-characteristic and characteristic components. Furthermore, there is essentially no phase shift in both directions as opposed to the non-Galerkin approach. As a result, the coarse grid correction is second and third order accurate in the characteristic and cross-characteristic components, respectively.

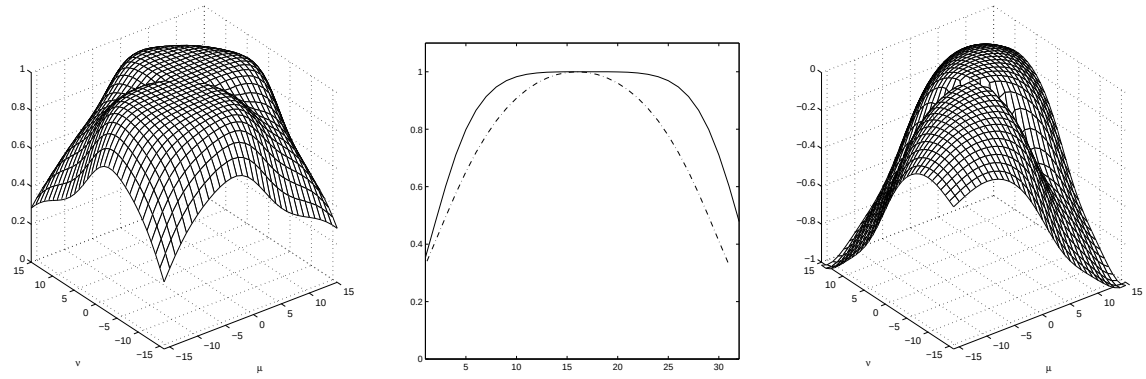

FIG. 11. *Spectrum of the Fourier transform of $D = p(G^H)^{-1} r L^h$ where G^H is obtained from the Galerkin approach to the entering flow problem. (a) $|\hat{D}_{\mu,\nu}(1,1)|$, (b) $|\hat{D}_{\mu,\nu}(1,1)|$, $\mu = \nu$ (solid line) and $\mu = -\nu$ (dashed line) (c) Scaled phase angle of $\hat{D}_{\mu,\nu}(1,1)$.*

Figure 11(a) shows that $|\hat{D}_{\mu,\nu}(1,1)| \approx 1$, for $\mu, \nu \approx 0$ in all directions. In particular, Figure 11(b) shows the values of $|\hat{D}_{\mu,\nu}(1,1)|$ in the characteristic (solid line) and cross-characteristic directions (dashed line) which verify the results of Theorem 4.4. Figure 11(c) shows the scaled values of the phase angles, $\frac{\theta}{(\mu+\nu)\pi h}$. Again for $\mu, \nu \approx 0$ in all directions, there is essentially no phase error.

Figure 12(a) and (b) show the contour plots of the fine grid error (dashed line) and the interpolated coarse grid error (solid line) for the entering flow and recirculating flow problems, respectively. Both results agree with the phase analysis that the interpolated coarse grid errors match accurately with the fine grid errors.

4.4. Summary. In practice, the Runge-Kutta CGC approach is appealing since it is simple and the same smoothing method can be used on all the coarse grids. However, such coarse grid correction is dispersive and oscillations generated can slow down multigrid convergence. For the exact CGC, direct discretization approach, the same smoothing method can also be used on all the coarse grids. Since exact coarse grid solve is used, the dispersive effect is much improved. However, the coarse grid correction is only first order accurate, leading to slower convergence. For the Galerkin approach, the

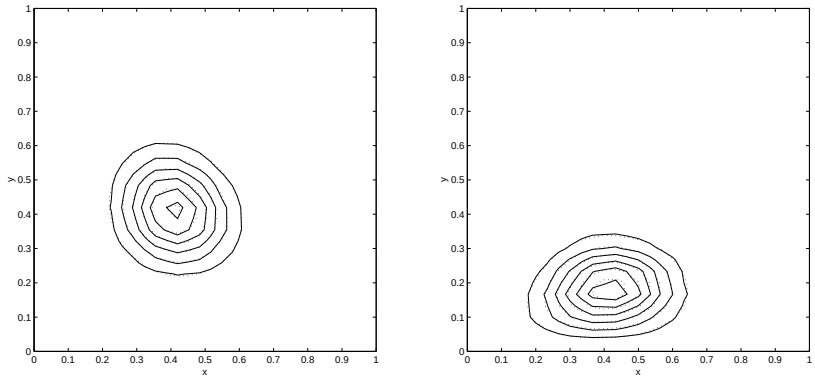

FIG. 12. *Contour plots of the fine grid error (dashed line) and the interpolated coarse grid error (solid line) for (a) the entering flow, and (b) the recirculating flow,.*

coarse grid correction is more accurate, and hence the resulting multigrid convergence should be like the elliptic case.

We note that although our analysis suggests that the Galerkin approach has the least phase error, in practice, however, there are several issues to be addressed. It has been observed that the Galerkin coarse grid operator on the coarse grids become more and more like the central finite difference discretization and hence leads to stability problems. To remedy this problem, carefully designed interpolation is needed, for instance, operator-dependent interpolations [15, 39], such that the resulting Galerkin coarse grid operator is stable. An ideal case would be that the Galerkin coarse grid operator coincides with the one by direct discretization. The construction of such interpolations, however, requires further research.

5. Applications. In the classical Fourier analysis based on first differential approximation [4, 11, 12], the convergence factor of multigrid methods for solving convection dominated problems using direct discretization as coarse grid operators is at best 0.5. In this analysis, the effect of the interpolation and restriction operators are ignored. However, as we have seen, the phase error property of the coarse grid correction process is coupled with the coarse grid operator as well as the interpolation and restriction operators. In this section, we show that our phase velocity analysis can explain the fast convergence of two multigrid methods which use direct discretization coarse grid operator and upwind-type interpolation and restriction.

5.1. Modified Runge-Kutta CGC method. In section 3.2, we show that the convergence of the multigrid methods based on the wave propagation approach is slowed down by the dispersion effect. To fix this problem, an upwind-type interpolation and restriction are proposed in [23]. More precisely, the upwind-biased residual restriction operator, r, can be defined as:

$$r(d_i^h) = \frac{1}{2}(d_i^h + d_{i-1}^h), \tag{12}$$

where d^h is the fine grid residual. Similarly, the interpolation of a coarse grid function v^H is given by:

$$(pv^H)_{2i} = (pv^H)_{2i+1} = v_{2i}^H.$$

Moreover, the coarse grid update formula is also modified:

$$u^{n+1} = \bar{u}^h + p(\bar{u}^H - ru^n),$$

where $\bar{u}^h$ and $\bar{u}^H$ are the approximate solution after smoothing on the fine and coarse grid, respectively. When applying this multigrid method to solving the 1D model equation (3), the iteration matrix M of a two-level method is given by:

$$M = [I + p_{odd}r - \lambda(p_{even} + p_{odd})L^H r](I - \lambda L^h) - p_{odd}r,$$

where

$$p_{odd} = \begin{bmatrix} 0 & & & \\ 1 & & & \\ & 0 & & \\ & 1 & & \\ & & \ddots & \end{bmatrix}, \qquad p_{even} = \begin{bmatrix} 1 & & & \\ 0 & & & \\ & 1 & & \\ & 0 & & \\ & & \ddots & \end{bmatrix}, \qquad r = p_{even}^T.$$

In this case, the iteration matrix cannot be written as a product of two matrices. Thus, we will compute the eigenvalues of M directly.

LEMMA 5.1. *The Fourier transformed iteration matrix is given by*

$$\hat{M}_\mu = [I + (\hat{p}_{odd})_\mu (\hat{r})_\mu - \lambda((\hat{p}_{odd})_\mu + (\hat{p}_{even})_\mu)\hat{L}_\mu^H (\hat{r})_\mu](I - \lambda \hat{L}_\mu^h) - (\hat{p}_{odd})_\mu (\hat{r})_\mu,$$

where $\hat{L}_\mu^h$ and $\hat{L}_\mu^H$ as in (4) and

$$(\hat{p}_{even})_\mu = \frac{1}{\sqrt{2}} \begin{bmatrix} e^{-\mu\pi hi} \\ e^{-\mu\pi hi} \end{bmatrix}, \qquad (\hat{p}_{odd})_\mu = \frac{1}{\sqrt{2}} \begin{bmatrix} 1 \\ -1 \end{bmatrix}, \qquad (\hat{r})_\mu = (\hat{p}_{even})_\mu^T.$$

Suppose the largest time step size is taken, i.e. λ=1.0. We have the following result.

THEOREM 5.2. *The eigenvalues of $\hat{M}_\mu$ are 0 and $e^{-4\mu\pi hi}$.*

Proof. Simplifying the formula for $\hat{M}_\mu$ in Lemma 5.1 with $\lambda = 1.0$, we obtain

$$\hat{M}_\mu = e^{-3.5\mu\pi hi} \begin{bmatrix} \cos(\mu\pi h/2) & -\cos(\mu\pi h/2) \\ i\sin(\mu\pi h/2) & -i\sin(\mu\pi h/2) \end{bmatrix}.$$

By direct calculation, the eigenvalues of $\hat{M}_\mu$ are 0 and $e^{-4\mu\pi hi}$. □

By Theorem 5.2, it is clear that the phase velocity is 4 for any wave number μ. Hence there is no dispersion, as opposed to the standard Runge-Kutta multigrid method discussed in Section 3.2. In other words, the numerical error will propagate with a speed of 4. Numerical results showing fast convergence of this multigrid method can be found in [23].

5.2. Modified Exact CGC, direct discretization method. Linear interpolation and full weighting are used in the exact coarse grid correction, direct dicretization approach in Section 3.3. Here we use the upwind restriction defined in (12) instead. Since the first differential approximate analysis [4] ignores the interpolation and restriction operators completely, it would have concluded that the modified multigrid method would not be any better than the one using full weighting. However, as indicated in the numerical section [4, page 84], such restriction indeed leads to better convergence, but no explanation was given. We can explain this phenomenon from the phase velocity perspective. In particular, we shall show that there is no phase error in the coarse grid correction.

THEOREM 5.3. *The (1,1) entry of the Fourier transformed coarse grid correction matrix is*

$$\hat{C}_\mu(1,1) = s_\mu^2.$$

Proof. Denote the upwind restriction operator by $\tilde{r}$. Using the Fourier transform results in Section 3.3 and the last section, the Fourier transform of the coarse grid correction matrix is given by:

$$\begin{aligned} \hat{C}_\mu &= I - \hat{p}_\mu (\hat{L}_\mu^H)^{-1} \hat{\tilde{r}}_\mu \hat{L}^h \\ &= I - \sqrt{2} \begin{bmatrix} c_\mu^2 \\ -s_\mu^2 \end{bmatrix} \frac{2h}{1 - e^{-2\mu\pi hi}} \frac{1}{2\sqrt{2}} \begin{bmatrix} e^{-\mu\pi hi} + 1 & e^{-\mu\pi hi} - 1 \end{bmatrix} \frac{1}{h} \begin{bmatrix} 1 - e^{-\mu\pi hi} & 0 \\ 0 & 1 + e^{-\mu\pi hi} \end{bmatrix} \\ &= \begin{bmatrix} s_\mu^2 & c_\mu^2 \\ s_\mu^2 & c_\mu^2 \end{bmatrix}. \end{aligned}$$

□

As opposed to the results in Section 3.3, if appropriate interpolation and/or restriction is used, there is no phase error in the coarse grid correction process when direct discretization is used. Hence, fast multigrid convergence is expected. In fact, the Fourier transformed coarse grid correction matrix coincides with the one derived in the case of Poisson equation.

6. Numerical results. In the following, we compare the effects of different coarse grid corrections on the convergence of multigrid V-cycle. The first example is the steady state solution of the one-dimensional linear wave equation:

$$u_t + u_x = 0.$$

Euler's method is used as the smoother for the approaches with CFL number $\lambda = 0.5$. Linear interpolation and full weighting restriction are used between grids. The multigrid V-cycle iterations stop when the relative residual norm is less than 10^{-6}. To obtain convergence, zero boundary condition is used.

h	Inexact	Non-Galerkin	Galerkin
1/32	31 (35)	13 (16)	8 (11)
1/64	44 (52)	9 (16)	5 (12)
1/128	73 (83)	6 (17)	3 (12)
1/256	141 (144)	5 (17)	3 (12)

TABLE 1

Number of two-grid V-cycles for the 1D linear wave equation using Runge-Kutta CGC (inexact), Exact CGC, direct discretization (non-Galerkin), and Galerkin CGC (Galerkin).

The number of multigrid V-cycles are shown in Table 1. We denote the Runge Kutta CGC, Exact CGC with direct discretization and Galerkin CGC by inexact, non-Galerkin and Galerkin, respectively. To verify the results of the previous sections, we use two multigrid levels and consider a smooth initial guess and a square wave initial guess (in parenthesis). The results show that the number of multigrid V-cycles taken by the inexact coarse grid correction increases as mesh size decreases; thus we do not observe the classical mesh-independent convergence. Moreover, the convergence is slow due to the dispersion of the inexact coarse grid solve. Both non-Galerkin and Galerkin approaches, which use exact coarse grid solve, show much better convergence. However, due to the phase error occurred at coarse grid correction, the non-Galerkin approach is not as efficient as the Galerkin approach. We also note that the square wave initial guess, which consists of more significant intermediate high frequencies, has more severe dispersive effects on the multigrid convergence. Qualitatively speaking, both initial guesses give very similar results and hence we will show only the results using the smooth initial guess in the following tests.

	Inexact					Non-Galerkin				
h	2	3	4	5	6	2	3	4	5	6
1/32	31	35	39			13	25	34		
1/64	44	43	45	51		9	22	37	46	
1/128	73	52	58	61	61	6	13	31	49	55
1/256	141	83	64	72	72	5	9	19	40	59

TABLE 2

Number of multigrid V-cycles with 2 to 6 number of coarse grids for the 1D linear wave equation using inexact and non-Galerkin coarse grid corrections.

The same qualitative results hold when more coarse grids are used. Table 2 shows the multilevel convergence of the inexact and non-Galerkin coarse grid correction approaches. The Galerkin approach requires different smoothing parameters on the coarse grids since the coarse grid operators are changed from grid to grid, and hence it is not tested in this case. For the inexact coarse grid correction approach, the convergence should, in principle, have been improved by using more coarse grids based on the result of Gustafsson and Lötstedt (cf. Theorem 2.1). This is indeed true when the mesh size is very small ($h = 1/256$) since the small wave number components are more dominant in the initial guess. But when the coarse grid gets smaller, the convergence starts to deteriorate. For the non-Galerkin approach, the

multigrid convergence also starts to deteriorate on the coarser grids due to the shift of the coarse grid errors which is more serious with larger mesh size. Thus the phase errors in the coarse grid correction cause a more serious damage to the multigrid convergence with more coarse grid levels.

We next consider the model entering flow and recirculating flow problems in two dimensions (cf. Section 4). For the entering flow problem, 2 pre and 2 post Euler's smoothing are used for all the coarse grid correction approaches and the CFL number, $\lambda = 0.25$. For the recirculating flow problem, we find that the smoothing effect of Euler's method is very poor. Thus, we use Gauss-Seidel for the presmoothing and backward Gauss-Seidel for the postsmoothing. As noted in Section 4, special orderings are often used to enhance convergence. But here, our primary focus is on the coarse grid correction part and therefore natural ordering is used. Linear interpolation and full weighting restriction are used for all cases; except for the singular point (0.5,0.5) of the recirculating flow problem, injection is used instead [12].

	Entering flow			Recirculating flow		
h	Inexact	Non-Galerkin	Galerkin	Inexact	Non-Galerkin	Galerkin
1/32	28	13	7	63	14	6
1/64	41	13	5	72	14	6
1/128	70	11	5	84	14	7
1/256	134	9	5	> 100	14	8

TABLE 3

Number of two-grid V-cycles for the 2D entering and recirculating flow problems using inexact, non-Galerkin, and Galerkin coarse grid corrections.

The two-grid results are shown in Table 3. As in the 1D case, the convergence of the Runge-Kutta coarse grid correction approach is slow because of the dispersion effect. The convergence of the non-Galerkin and Galerkin approaches are shown to be insensitive to the mesh size. We also remark that although our phase velocity analysis cannot be applied to variable coefficient cases, the numerical results of the recirculating flow indicate that the same conclusions hold for the different coarse grid correction approaches.

7. Conclusions. We have demonstrated that phase velocity analysis is a useful tool to analyze multigrid methods for convection dominated problems, and brings more insight into the efficiency of different coarse grid correction approaches. In contrast with the elliptic case where multigrid convergence is governed by smoothing of high frequencies and coarse grid correction of the smooth frequencies, we have shown that it also depends on phase velocity accuracy on coarse grids for hyperbolic problems.

For Runge-Kutta coarse grid correction, the propagation of smooth waves is accelerated by using coarse grids. However, dispersion occurs in the coarse grid correction process, which slows down substantially the multigrid convergence. The exact coarse grid solve approach does not rely on wave propagation and hence dispersion is not an issue. However, for the use of the discretization matrix as the coarse grid operator, there is a phase shift error in the coarse grid error which deteriorates the multigrid convergence. The Galerkin approach has the advantage of maintaining small shift error in the coarse grid correction. However, one needs to form the coarse grid operators on every grids, and hence to determine new sets of parameters, e.g. time-step size, for the smoother to obtain good smoothing efficiency.

We have addressed the issue of phase velocity analysis of multigrid methods for convection dominated problems. However, the design of new multigrid methods which possess good phase velocity property require further investigation.

REFERENCES

[1] J. Bey and G. Wittum. Downwind numbering: Robust multigrid for convection-diffusion problems. *Appl. Numer. Math.*, 23:177–192, 1997.

[2] J. Bramble, J. Pasciak, J. Wang, and J. Xu. Convergence estimates for multigrid algorithms without regularity assumptions. *Math. Comp.*, 57:23–45, 1991.

[3] A. Brandt. Multi-level adaptive solutions to boundary-value problems. *Math. Comp.*, 31:333–390, 1977.

[4] A. Brandt. Multigrid solvers for non-elliptic and singular-perturbation steady-state problems. Department of Applied Mathematics, The Weizmann Institute of Science, 76100 Rehovot, Israel, 1981.

[5] A. Brandt. Guide to multigrid development. In W. Hackbusch and U. Trottenberg, editors, *Multigrid Methods*, volume 960 of *Lectures Notes in Mathematics*, pages 220–312. Springer-Verlag, Berlin, 1982.

[6] A. Brandt. *Multigrid Techniques: 1984 Guide with Applications to Fluid Dynamics*. GMD–Studien Nr. 85. Gesellschaft für Mathematik und Datenverarbeitung, St. Augustin, 1984.

[7] A. Brandt. Rigorous local mode analysis of multigrid. In *Proceedings of the Fourth Copper Mountain Conference on Multigrid Methods*, Copper Mountain, CO, 1989.

[8] A. Brandt. Rigorous quantitative analysis of multigrid: I. constant coefficients two level cycle with l_2 norm. *SIAM J. Numer. Anal.*, 31:1695–1730, 1994.

[9] A. Brandt. Barriers to achieving textbook multigrid efficiency in CFD. Technical Report Interim report no. 32, NASA/CR-1998-207647, ICASE, NASA, 1998.

[10] A. Brandt and I. Yavneh. On multigrid solution of high-Reynolds incompressible entering flows. *J. Comput. Phys.*, 101:151–164, 1992.

[11] A. Brandt and I. Yavneh. On multigrid solution of high-reynolds incompressible entering flows. *J. Comput. Phys.*, 101:151–164, 1992.

[12] A. Brandt and I. Yavneh. Accelerated multigrid convergence and high-Reynolds recirculating flows. *SIAM J. Sci. Comput.*, 14:607–626, 1993.

[13] T. F. Chan and W. L. Wan. Robust multigrid methods for elliptic linear systems. *J. Comput. Appl. Math.*, 123:323–352, 2000.

[14] T.F. Chan and H. Elman. Fourier analysis of iterative methods for elliptic problems. *SIAM Review*, 31:20–49, 1989.

[15] J. E. Dendy, Jr. Black box multigrid for nonsymmetric problems. *Appl. Math. Comput.*, 13:261–283, 1983.

[16] B. Gustafsson and P. Lötstedt. Analysis of the multigrid method applied to first order systems. In J. Mandel et al., editor, *Proceedings of the Fourth Copper Mountain Conference on Multigrid Methods*, pages 181–233, Philadelphia, PA, 1989. SIAM.

[17] W. Hackbusch. Multigrid convergence for a singular perturbation problem. *Lin. Alg. Appl.*, 58:125–145, 1984.

[18] W. Hackbusch. *Multi-grid Methods and Applications*. Springer-Verlag, Berlin, 1985.

[19] W. Hackbusch and T. Probst. Downwind gauss-seidel smoothing for convection dominated problems. *Numer. Lin. Alg. Appl.*, 4:85–102, 1997.

[20] A. Jameson. Solution of the Euler equations for two dimensional transonic flow by a multigrid method. *Appl. Math. Comp.*, 13:327–355, 1983.

[21] A. Jameson. Computational transonics. *Comm. Pure Appl. Math.*, 41:507–549, 1988.

[22] A. Jameson, W. Schmidt, and E. Turkel. Numerical solutions of the Euler equations by finite volume methods using Runge-Kutta time-stepping schemes. *AIAA paper 81-1259*, 1981.

[23] A. Jameson and W.L. Wan. Monotonicity preserving and total variation diminishing multigrid time stepping methods. Technical Report CS-2001-11, Department of Computer Science, University of Waterloo, April 2001.

[24] D. C. Jespersen. A time-accurate multiple-grid algorithm. AIAA paper 85-1493-CP, 1985.

[25] Klaus Johannsen. Robust smoothers for convection-diffusion problems. Technical report, Institute for Computer Applications, University of Stuggart, 1999.

[26] P. Lötstedt and B. Gustafsson. Fourier analysis of multigrid methods for general systems of PDEs. *Math. Comp.*, 60:473–493, 1993.

[27] R. H. Ni. A multiple-grid scheme for solving the euler equations. *AIAA*, 20:1565–1571, 1982.

[28] A. Reusken. Multigrid with matrix-dependent transfer operators for a singular perturbation problem. *Computing*, 50:199–211, 1993.

[29] A. Reusken. Fourier analysis of a robust multigrid method for two-dimensional convection-diffusion equations. *Numer. Math.*, 71:365–398, 1995.

[30] K. Stüben and U. Trottenberg. Multigrid methods: Fundamental algorithms, model problem analysis and applications. In W. Hackbusch and U. Trottenberg, editors, *Multigrid Methods, Proceedings, Köln-Porz, 1981*, Lecture Notes in Mathematics 960, pages 1–176, Berlin, 1982. Springer-Verlag.

[31] U. Trottenbery, C. Oosterlee, and A. Schüller. *Multigrid.* Academic Press, 2001.

[32] R. Vichnevetsky and J. Bowles. *Fourier Analysis of Numerical Approximations of Hyperbolic Equations.* SIAM, Philadelphia, 1982.

[33] Feng Wang and Jinchao Xu. A crosswind block iterative method for convection-dominated problems. *SIAM J. Sci. Comput.*, 21:620–645, 1999.

[34] P. Wesseling. *An Introduction to Multigrid Methods.* Wiley, Chichester, 1992.

[35] R. Wienands and C.W. Oosterlee. On three-grid fourier analysis for multigrid. *SIAM J. Sci. Comput.*, 23:651–671, 2001.

[36] J. Xu. Iterative methods by space decomposition and subspace correction. *SIAM Review*, 34:581–613, 1992.

[37] N. N. Yanenko and Y. I. Shokin. Correctness of first differential approximations of difference schemes. *Doklady Akad. Nauk SSSR*, 182(4):1215–1217, 1968.

[38] I. Yavneh. Coarse-grid correction for nonelliptic and singular perturbation problems. *SIAM J. Sci. Comput.*, 19:1682–1699, 1998.

[39] P. M. De Zeeuw. Matrix-dependent prolongations and restrictions in a blackbox multigrid solver. *J. Comp. Appl. Math.*, 33:1–27, 1990.